Article

Amyloid-like Behavior in Abiotic, Amphiphilic Foldamers

Valerie J. Bradford, and Brent L. Iverson

J. Am. Chem. Soc., **2008**, 130 (4), 1517-1524 • DOI: 10.1021/ja0780840

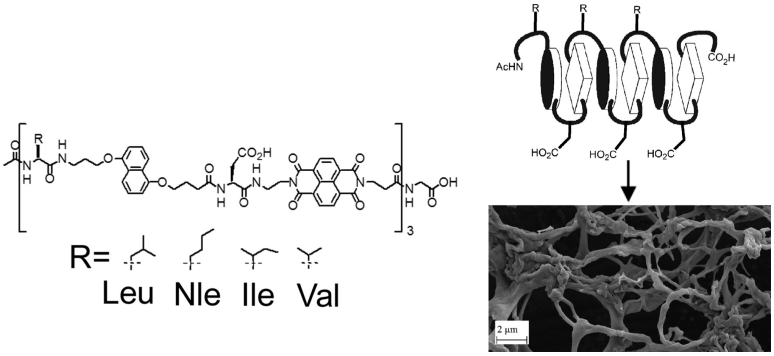

More About This Article

Additional resources and features associated with this article are available within the HTML version:

- Supporting Information
- Links to the 5 articles that cite this article, as of the time of this article download
- Access to high resolution figures
- Links to articles and content related to this article
- Copyright permission to reproduce figures and/or text from this article

View the Full Text HTML

J|A|C|S
ARTICLES
Published on Web 01/04/2008

Amyloid-like Behavior in Abiotic, Amphiphilic Foldamers

Valerie J. Bradford and Brent L. Iverson*

Department of Chemistry and Biochemistry, The University of Texas at Austin, Texas 78712

Received October 22, 2007; E-mail: biverson@mail.utexas.edu

Abstract: Previously, we reported an abiotic amphiphilic foldamer that, upon heating, undergoes an irreversible conformational change to a highly aggregated state (Nguyen, J.Q.; Iverson, B.L. *J. Am. Chem. Soc.* **1999**, *121*, 2639−2640.). Herein, we extend this work through the study of a series of structurally related amphiphilic foldamers and present a more refined model of their conformational switching behavior. Prior to heating, all foldamers of the series exhibited spectral characteristics consistent with folding in the pleated, stacked geometry characteristic of this class of foldamer. Following heating at 80 °C, three of the four molecules exhibited irreversible aggregation to produce hydrogels. The hydrogels were characterized by rheology measurements, and circular dichroism spectra revealed that hydrogel formation was dependent on highly ordered intermolecular assembly, conceptually analogous to protein amyloid formation. Hydrogel formation had the effect of amplifying the subtle structural differences between molecules, as the three amphiphilic foldamer constitutional isomers that formed hydrogels upon heating displayed significant differences in hydrogel properties. Taking a global view, our results indicate that amyloid-like behavior is not unique to proteins but may be a relatively general property of amphiphilic folding molecules in aqueous solution.

Introduction

There is a growing appreciation for the importance of alternative protein conformations. Biological activity is not restricted to globular folded structures because the polymeric nature of proteins combined with the unique conformational properties of the polypeptide backbone can lead to structured aggregates that have important consequences *in vivo* and *in vitro*. [1] In particular, self-assembled and ordered protein fibrillar aggregates are symptomatic of an expanding list of diseases that now includes systemic amyloidoses,[2] Alzheimer's disease,[3] Huntington's disease,[4] spongiform encephalopathies,[5] Parkinson's disease,[6] and Type II diabetes.[7]

The common theme among the amyloid diseases is the presence of partially unfolded or misfolded proteins that self-assemble into *highly ordered* β-structured protofibrils followed by further assembly into amyloid fibrils.[8] This conformational change and ordered assembly is irreversible, and the amyloid fibrils can form protein precipitates *in vivo*. Interestingly, in the case of Alzheimer's disease and transthyretin amyloidoses, there is growing evidence that the protofibrils are the toxic species rather than the mature amyloid precipitates.[9]

Many proteins have been shown to undergo the transformation to self-assembled fibrils.[10] The requisite cross-β fiber assembly is potentially accessible to all polypeptides by virtue of intrachain and interchain interactions of amide backbones. Although the main-chain interactions determine the overall structural theme of the amyloid, the side-chain interactions of the specific polypeptide sequence determine the variations in the fibrillar structure. These structural variations, due to polypeptide sequence coupled with structural variations from subtle changes in solution conditions, have led to the conclusion that although the cross-β fold and ordered self-assembly may be thermodynamically favored, the exact structural details are determined by kinetic accessibility.[11] There have been many systems designed to display this amyloid-like behavior, although almost all have utilized protein-derived and *de novo* designed peptides.[12]

Interestingly, recent studies have shown that the aggregation rates of polypeptides (unlike folding of the native structure) can be predicted using a simple "polymer" model.[13] The obvious difference between non-natural polymers and proteins is that proteins exhibit exquisitely well-defined native folds, which can persist in solution (without aggregation) because they represent local free energy minima. The cross-β aggregates of these same polypeptides correspond to different, more global free energy minima with entirely different sets of ordered conformations.

(1) (a) Fowler, D. M.; Koulov, A. V.; Balch, W. E.; Kelly, J. W. *Trends Biochem. Sci.* **2007**, *32*, 217−224. (b) Obici, L.; Perfetti, V.; Palladini, G.; Moratti, R.; Merlini, G. *Biochim. Biophys. Acta* **2005**, *1753*, 11−22.
(2) Merlini, G.; Westermark, P. *J. Intern. Med.* **2004**, *255*, 159−178.
(3) Finder, V. H.; Glockshuber, R. *Neurodegenerative Dis.* **2007**, *4*, 13−27.
(4) Ross, C. A. *Neuron* **2002**, *35*, 819−822.
(5) Chakraborty, C.; Nandi, S.; Jana, S. *Curr. Pharm. Biotechnol.* **2005**, *6*, 167−177.
(6) Cookson, M. R. *Annu. Rev. Biochem.* **2005**, *74*, 29−52.
(7) Hoeppener, J. W. M.; Lips, C. J. M. *Int. J. Biochem. Cell B* **2006**, *38*, 726−736.
(8) Binder, W. H.; Smrzka, O. W. *Angew. Chem., Int. Ed.* **2006**, *45*, 7324−7238.
(9) (a) Kayed, R.; Head, E.; Thompson, J. L.; McIntire, T. M.; Milton, S. C.; Cotman, C. W.; Glabe, C. G. *Science* **2003**, *300*, 486−489. (b) Taylor, B. M.; Sarver, R. W.; Fici, G.; Poorman, R. A.; Lutzke, B. S.; Molinari, A.; Kawabe, T.; Kappenman, K.; Buhl, A. E.; Epps, D. E. *J. Protein Chem.* **2003**, *22*, 31−40. (c) Reixach, N.; Deechongkit, S.; Jiang, X.; Kelly, J. W.; Buxbaum, J. N. *Proc. Natl. Acad. Sci. U.S.A.* **2004**, *101*, 2817−2822.
(10) Dobson, C. M. *Nature* **2003**, *426*, 884−890.
(11) Chiti, F.; Dobson, C. M. *Annu. Rev. Biochem.* **2006**, *75*, 333−366.

There are likely to be partial unfolding conformations lying adjacent to, or between, these ordered states on the free energy landscape. [14]

The contrasting behavior of non-natural polymers and proteins leads to some interesting questions. First, is it possible to create an abiotic (i.e., non-polypeptide) system capable of exhibiting amyloid-like behavior involving two free energy minima, both of which exhibit a great deal of conformational order, the more thermodynamically stable of which is the ordered aggregate? If so, what characteristics of such an abiotic system modulate behavior and properties?

Previously, we reported an abiotic amphiphilic foldamer (cmpd **1**) that upon heating undergoes an irreversible conformational change leading to formation of a hydrogel.[15] Herein, we report the synthesis and characterization of a series of related foldamers designed to probe the effect of hydrophobic side chain structure on this behavior. The results lead to a more refined model of the conformational switching of this series of foldamers in which the hydrogel state of our foldamer is shown to be the result of the *highly ordered assembly* of alternatively folded molecules, conceptually analogous to protein amyloid formation.

Background

There are now many reports of α-amino acid peptide or protein-derived hydrogels that arise from the ordered aggregation of self-assembled fibers.[16] The highly ordered assembly of cyclic peptides has also been used to produce interesting structures analogous to pores.[17] On the abiotic side, an amphiphilic *β*-peptide foldamer was shown to self-assemble into a lyotropic phase.[18] There are also a growing list of reports involving abiotic foldamers that undergo a conformational change in response to some external stimulus.[19] However, to the best of our knowledge, the previously reported amphiphilic foldamer **1** is the only foldamer reported to exhibit conformational switching combined with hydrogel formation behavior.

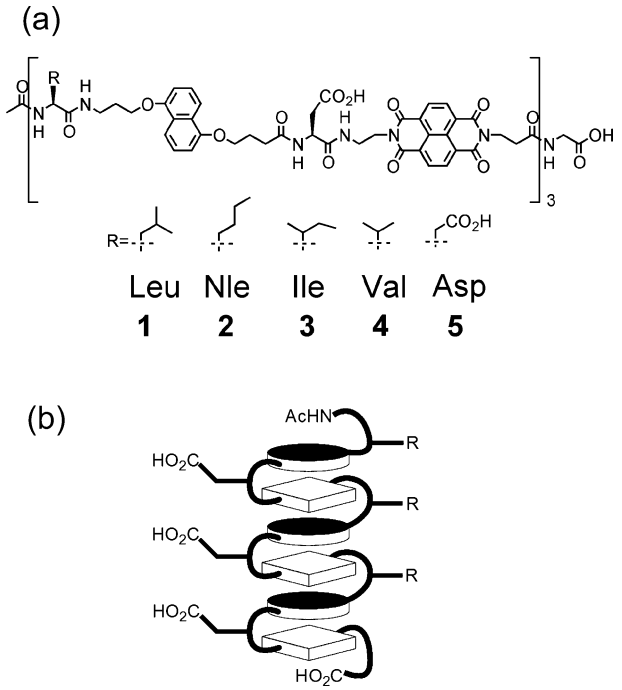

Figure 1. (a) Structure of amphiphilic aedamers **1**−**5** and (b) cartoon of the folded conformation.

Foldamer **1** belongs to a class of molecules we refer to as *aedamers*, named for the *a*romatic *e*lectron *d*onor-*a*cceptor fold*a*m*er* design that enables their folding into a pleated structure in water driven by the complementary electrostatics and hydrophobics of alternating electron-rich 1,5-dialkoxynapthalene (DAN) and electron-deficient 1,4,5,8-napthalenetetracarboxilic acid diimide (NDI) aromatic units. The aedamer aromatic units are most often linked with amino acids. Folded aedamers have been characterized using a number of spectroscopic techniques and display a characteristic charge transfer absorbance in the visible region that gives aqueous solutions of folded aedamers the purple color characteristic of a fine merlot, even though the component DAN and NDI units are not colored in the visible region when dissolved individually.[20]

The amphiphilic aedamer **1** was constructed with linkers between aromatic units that contained one amino acid, which alternated between leucine and aspartic acid. When folded, the hydrophobic leucine residues are in position to reside on one side, and the negatively charged aspartate residues are in position to reside on the opposite side of the pleated, stacked core as shown in Figure 1.

(12) (a) Hamley, I. W. *Angew. Chem., Int. Ed.* **2007**, *46*, 8128−8147. (b) Teplow, D. B. *Amyloid* **1998**, *5*, 121−142. (c) Makin, O. S.; Atkins, E.; Sikorski, P.; Johansson, J.; Serpell, L. C. *Proc. Natl. Acad. Sci. U.S.A.* **2005**, *102*, 315−320. (d) Ciani, B.; Hutchinson, E. G.; Session, R. B.; Woolfson, D. N. *J. Biol. Chem.* **2002**, *277*, 10150−10155. (e) Mimna, R.; Camus, M. S.; Schmid, A.; Tuschscherer, G.; Lashuel, H. A.; Mutter, M. *Angew. Chem., Int. Ed.* **2007**, *46*, 2681−2684. (f) Chen, P. *Colloids Surf. A* **2005**, *261*, 3−24. (g) Matsumura, S.; Uemura, S.; Mihara, H. *Chem. Eur. J.* **2004**, *10*, 2789−2794. (h) Aggeli, A.; Nyrkova, I. A.; Bell, M.; Harding, R.; Carrick, L.; McLeish, T. C. B.; Semenov, A. N.; Boden, N. *Proc. Natl. Acad. Sci. U.S.A.* **2001**, *98*, 11857−11862. (i) Wang, K.; Keasling, J. D.; Muller, S. J. *Int. J. Biol. Macromol.* **2005**, *36*, 232−240. (j) Ray, S.; Drew, M. G. B.; Das, A. K.; Banerjee, A. *Supramol. Chem.* **2006**, *18*, 455−464. (k) Deechongkit, S.; Powers, E. T.; You, S. L.; Kelly, J. W. *J. Am. Chem. Soc.* **2005**, *127*, 8562−8570. (l) Mesquida, P.; Riener, C. K.; MacPhee, C. E.; McKendry, R. A. *J. Mater. Sci.* **2007**, *18*, 1325−1331. (m) Hirata, A.; Sugimoto, K.; Konno, T.; Morii, T. *Bioorg. Med. Chem. Lett.* **2007**, *17*, 2971−2974. (n) Kammerer, R. A.; Kostrewa, K.; Zurdo, J.; Detken, A.; Garcia-Echeverria, C.; Green, J. D.; Muller, S. A.; Meier, B. H.; Winkler, F. K.; Dobson, C. M.; Steinmetz, M. O. *Proc. Natl. Acad. Sci. U.S.A.* **2004**, *101*, 4435−4440.
(13) (a) Chiti, F.; Stefani, M.; Taddel, N.; Ramponi, G.; Dobson, C. M. *Nature* **2003**, *424*, 805−808. (b) Tartaglia, G. G.; Cavalli, A.; Pellarin, R.; Caflisch, A. *Protein Sci.* **2004**, *13*, 1939−1941. (c) Meinhardt, J.; Tartaglia, G. G.; Pawar, A.; Christopeit, T.; Hortschansky, P.; Schroeckh, V.; Dobson, C. M.; Verdruscolo, M.; Fandrich, M. *Protein Sci.* **2007**, *16*, 1214−1222.
(14) Gregersen, N.; Bross, P.; Vang, S.; Christensen, J. H. *Annu. Rev. Genom. Hum. G.* **2006**, *7*, 103−124.
(15) Nguyen, J. Q.; Iverson, B. L. *J. Am. Chem. Soc.* **1999**, *121*, 2639−2640.
(16) (a) Chen, M.; Kisaalita, W. S. *Biosens. Bioelectron.* **2004**, *19*, 1075−1088. (b) Yang, Z.; Liang, G.; Wang, L.; Xu, B. *J. Am. Chem. Soc.* **2006**, *128*, 3038−3043. (c) Measey, T. J.; Schweitzer-Stenner, R. *J. Am. Chem. Soc.* **2006**, *128*, 13324 -13325. (d) Deming, T. J. *Soft Matter* **2005**, *1*, 28−35. (e) Shen, W.; Kornfield, J. A.; Tirrell, D. A. *Macromolecules* **2007**, *40*, 689−692. (f) Ramachandran, S.: Tseng, Y.; Yu, Y. B. *Biomacromolecules* **2005**, *6*, 1316−1321. (g) Schneider, J. P.; Pochan, D. J.; Ozbas, B.; Rajagopal, K.; Pakstis, L.; Kretsinger, J. *J. Am. Chem. Soc.* **2002**, *124*, 15030−15037. (h) Xu, C.; Kopecek, J. *Polym. Bull.* **2007**, *58*, 53−63. (i) Aggeli, A.; Bell, M.; Carrick, L. M.; Fishwick, C. W. G.; Harding, R.; Mawer, P. J.; Radford, S. E.; Strong, A. E.; Boden, N. *J. Am. Chem. Soc.* **2003**, *125*, 9619−9628.
(17) (a) Sánchez-Quesada, J.; Isler, M. P.; Ghadiri, M. R. *J. Am. Chem. Soc.* **2002**, *124*, 10004−10005. (b) Sánchez-Quesada, J.; Kim, H. S.; Ghadiri, M. R. *Angew. Chem., Int. Ed.* **2001**, *40*, 2503−2506.
(18) Pomerantz, W. C.; Abbott, N. L.; Gellman, S. H. *J. Am. Chem. Soc.* **2006**, *128*, 8730−8731.
(19) (a) Haldar, D.; Jiang, H.; Leger, J. M.; Huc, I. *Angew. Chem. Int. Ed.* **2006**, *45*, 5483−5486. (b) Seebach, D.; Hook, D. F.; Glattli, A. *Biopolymers* **2006**, *84*, 23−37. (c) Tanaka, H.; Bollot, G.; Mareda, J.; Litvinchuk, S.; Tran, D. H.; Sakai, N.; Matile, S. *Org. Biomol. Chem.* **2007**, *5*, 1369−1380. (d) Tanaka, H.; Litvinchuk, S.; Tran, D. H.; Bollot, G.; Mareda, J.; Sakai, N.; Matile, S. *J. Am. Chem. Soc.* **2006**, *128*, 16000−16001. (e) Balakrishnan, K.; Datar, A.; Zhang, W.; Yang, X.; Naddo, T.; Huang, J.; Zuo, J.; Yen, M.; Moore, J. S.; Zang, L. *J. Am. Chem. Soc.* **2006**, *128*, 6576−6577. (f) Liu, S.; Zavalij, P. Y.; Lam, Y. F.; Isaacs, L. *J. Am. Chem. Soc.* **2007**, *129*, 11232−11241. (g) Khan, A.; Kaiser, C.; Hecht, S. *Angew. Chem., Int. Ed.* **2006**, *45*, 1878−1881.
(20) Lokey, S.; Iverson, B. L. *Nature* **1995**, *375*, 303−305.

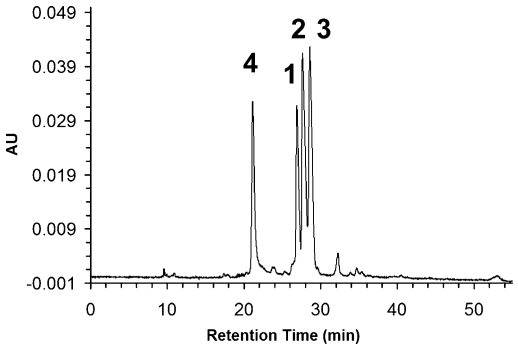

Figure 2. RP-HPLC chromatograph of co-injection of compounds **1**−**4**.

Upon heating, amphiphilic aedamer **1** undergoes an irreversible transition to a hydrogel state with significant loss of the charge-transfer absorbance. A mechanism of hydrogelation was proposed that involved partial unfolding of the initial pleated structure followed by hydrophobically driven aggregation to a "tangled" hydrogel state in analogy to non-natural polymers. The proposed mechanism took into account a well-defined, folded initial state, as any population of unfolded molecules should lead to hydrogel formation at room temperature (not observed). The "tangled" aggregate hydrogel final state, as originally described, was of unknown conformational order, and its properties were not investigated.[15]

Results

Aedamer Design and Synthesis. Figure 1 shows the series of aedamers synthesized to probe the effect of the hydrophobic linker amino acid residue on hydrogel properties of heated samples. In addition to the original leucine derivative, valine, isoleucine, and norleucine derivatives were synthesized to probe the influence of subtle structural changes on hydrogel properties. Note that compounds **1**−**3** are actually constitutional isomers.

All aedamer derivatives were synthesized using standard Fmoc solid-phase peptide synthesis methods using monomer units previously reported.[15] Experimental measures of the relative hydrophobicities of the aedamers **1**−**4** were investigated by a co-injection of the four compounds on reverse-phase HPLC as shown in Figure 2. The molecules eluted in the order **4** (Val), **1** (Leu), **2** (Nle), then **3** (Ile), indicating that the isoleucine derivative **3** was the most hydrophobic to a small degree, followed closely by the norleucine derivative **2** and leucine derivative **1**. Interestingly, valine compound **4** was significantly less hydrophobic than the other members of the series. To the best of our knowledge, this order of elution did not correspond exactly to any scale in the literature that includes norleucine.[21]

Light Scattering. Dynamic light scattering was measured for compounds **1**−**4** at 2.5 mM concentration in buffer prior to heating and analyzed assuming a globular protein structure and using the monomodal analysis of data provided by the manufacturer (Wyatt Technology Corp.). The resulting estimated molecular weights for compounds **1**−**4** are 239, 1.65×10^3, 210, and 340 kDa, respectively.

UV Spectroscopy. Face-centered stacking of the aromatic units of aedamers leads to pi molecular orbital overlap that causes a characteristic ∼50% hypochromism in the 382 nm NDI absorbance. To quantify the hypochromism associated with folding, ultraviolet spectra (UV) were recorded for the series of aedamers (∼15 μM) in aqueous buffer as well as in the presence of 2% (w/v) cetyl trimethylammonium bromide (CTAB) as shown in Figure 3. The positively charged CTAB detergent is known to unfold negatively charged aedamers by causing the unstacking of the aromatic units, so absorbance in CTAB is used to establish an absorbance value of unfolded aedamers for the hypochromism calculation. Observed hypochromism is reported as [(absorbance recorded in CTAB − absorbance recorded in buffer)/absorbance recorded in CTAB] × 100. The hypochromism values measured for compounds **1**−**5** are 51, 52, 52, 53, and 54%, respectively.

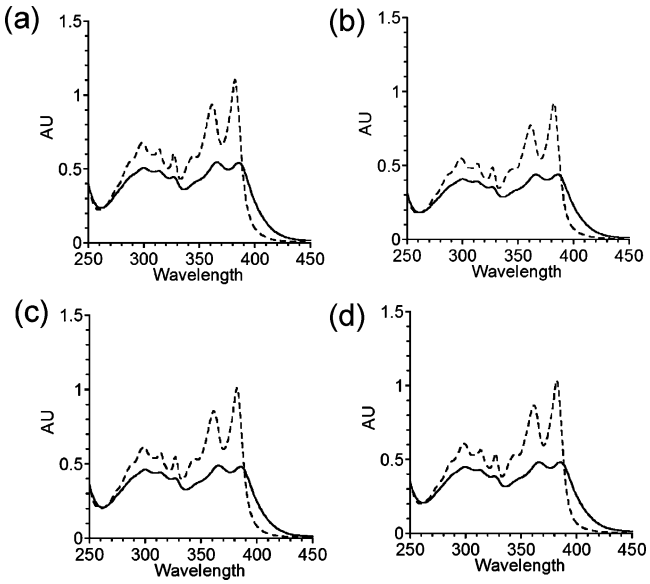

Figure 3. UV spectra of compounds **1**−**4** (a−d) with (---) and without (—) addition of 2% (w/v) CTAB indicating hypochromism.

Hydrogelation. Upon heating 2.0 mM solutions (∼0.50 wt %) of the compounds **1**−**4** at 80 °C for 1.5 h, compounds **1**−**3** formed viscous hydrogels. No hydrogel was seen in the case of the valine-containing **4**. Compounds **1**−**3** were also found to be capable of forming hydrogels at concentrations at 1.0 mM (∼0.25 wt %). Compound **4** did not produce a visible hydrogel even at its maximum solubility (∼5 mM) after heating at 95 °C for 2 h.

Visible Spectroscopy. Figure 4 shows the change in the visible region charge-transfer absorbance for compounds **1**−**4** both before and after heating. The degree of charge-transfer absorbance varied greatly with changes among the series. Compound **1** shows the smallest retention of charge-transfer absorbance after gelling, with only 28% of the original absorbance remaining. This loss in charge-transfer absorbance was accompanied by a shift in λ_{max} from 531 to 521 nm. Compound **2** retained 36% of the initial charge-transfer absorbance with a shift in λ_{max} from 529 to 511 nm. After accounting for light scattering, compound **3** retained 88% of the charge-transfer absorbance and a shift in λ_{max} from 525 to 502 nm. Unlike compounds **1**−**3**, the valine derivative **4** showed a 33% increase in the charge-transfer absorbance with a corresponding shift in λ_{max} from 518 to 514 nm. In all cases, the spectroscopic transitions that occurred upon heating were irreversible, even for compound **4**, as shown by repeated heating−cooling cycles.

(21) (a) Kovacs, J. M.; Mant, C. T.; Hodges, R. S. *Biopolymers* **2006**, *84*, 283−297. (b) Tossi, A.; Sandri, L.; Giangaspero, A. *Peptides* **2002**, *27*, 416−417.

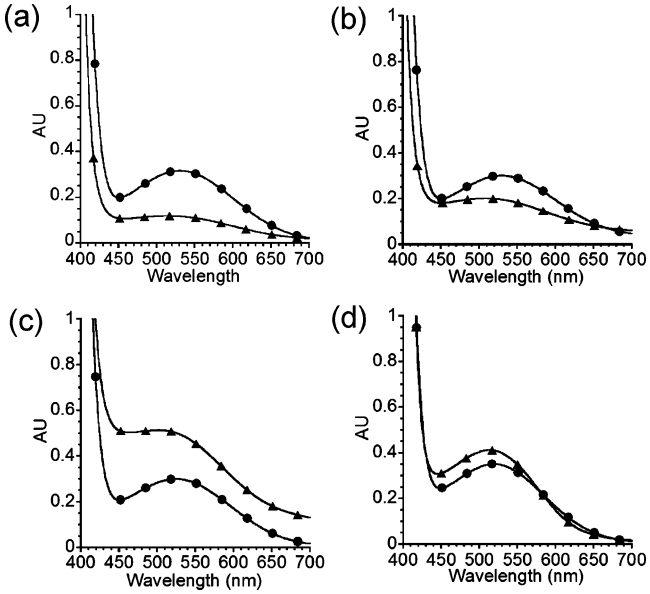

Figure 4. Visible spectrum of compounds **1**−**4** (a−d) before (●) and after (▲) heating at 80 °C.

Rheology. A variety of rheological experiments were performed to characterize compounds **1**−**4**, both before and after hydrogel formation. The absolute viscosity of a 4 mM solution of **1** was measured during heating from 25 °C to 80 °C, as shown in Figure 5a. Consistent with the light scattering results, the viscosity at room temperature for the solution of **1** was considerably greater than that of pure water (0.365 Pa•s versus 0.001 Pa•s). Interestingly, the viscosity of the solution decreases initially during heating, even approaching that of water. Once 80 °C is reached, the viscosity begins to increase rapidly corresponding to formation of hydrogel (data not shown) provided some pre-gelled material was placed in the rheology sample holder, which is presumably required because the rheology sample holder was entirely sealed and therefore did not allow for an air−water interface. Interestingly, compound **4**, although not forming a hydrogel, did show some increase in viscosity, from 0.038 Pa•s prior to heating to 0.143 Pa•s following heating at 80 °C.

Hydrogels were analyzed following seeding samples of the different aedamers with 10% pre-gelled material. Without seeding, the gels formed in the rheometer were not reproducible enough for quantitative comparison. We attributed this lack of reproducibility to the importance of the air−water interface in the nucleation step of the self-assembly process, which was altered in the absence of seeding because of the required silicon oil layer used to prevent evaporation in the rheometer.

Hydrogel behavior is indicated by a frequency-independent storage modulus (G'; a measure of elastic behavior) and loss modulus (G''; a measure of liquid behavior, i.e., the ability of the sample to flow). Figure 5b depicts a frequency sweep experiment in the linear viscoelastic regime at constant strain of 0.5% for compounds **1**−**3** at 4 mM concentration (∼1 wt %). Such frequency independence is consistent with gel behavior.[22] Both the storage and loss moduli of compound **4** were *not* frequency independent, as they both increased at higher frequency as shown in Figure 5c. For a direct comparison of elastic gel strength, the equilibrium storage moduli for compounds **1**−**4** at a frequency of 2.64 rad/s are 323, 652, 1400, and 0.22 Pa, respectively.

Another characteristic feature of hydrogel behavior is a larger storage modulus versus loss modulus ($G' > G''$). Values of the loss tangent, tan $\delta = G''/G'$, at a frequency of 2.64 rad/s for compounds **1**, **2**, and **3** are 0.096, 0.089, and 0.069, respectively. However, in the case of the valine derivative compound **4**, the loss modulus was found to be larger ($G'' > G'$) over the frequency range investigated. Again, these data are consistent with compounds **1**, **2**, and **3** exhibiting hydrogel behavior, whereas compound **4** does not.

Self-assembled hydrogels exhibit shear-thinning, that is a decline in absolute viscosity with an increase in shear rate due to disruptions of noncovalent cross-links within the gel.[16g,23] Figure 5d shows the representative shear-thinning behavior of leucine derivative compound **1** hydrogel. A significant decrease in viscosity with increasing shear rate was also observed for compounds **2** and **3**. Figure 5e shows a time sweep experiment at 25 °C where, after the gel formation of compound **1** is complete, 1000% strain is applied for 180 s, the strain was removed, and the storage and loss moduli were monitored. The hydrogel of compound **1** regained 94% of its initial elastic strength after only 15 min.

Circular Dichroism (CD) Spectroscopy. As a probe of possible higher order structure in the hydrogel state, CD spectra of the non-gelled and hydrogel form of compounds **1**−**4** were compared as shown in Figure 6. In addition to compounds **1**−**4**, a non-amphiphilic aedamer with all aspartate residues (compound **5**) was used as an important control molecule with well-characterized folding in aqueous solution, yet no ability to form a hydrogel state. As expected, the control compound **5** showed a relatively small signal in the carbonyl region (<250 nm) and nothing in the aromatic region (310−420 nm). There was no change in its CD spectrum observed upon heating.

Before heating, compound **1** gave a CD spectrum with only a very weak signal in the carbonyl region, similar in shape and intensity to the control compound **5.** After heating to the hydrogel state, a strong negative Cotton effect, centered at 206 nm, was observed followed by a strong positive Cotton effect centered at 231 nm. There are also less intense positive followed by negative Cotton effects in the aromatic region, centered at 328 and 393 nm, respectively. Compound **2** exhibited a strong negative Cotton effect at 223 nm with a relatively small maximum and minimum in the aromatic region at 316 and 342 nm. Compound **3** showed a strong positive Cotton effect at the lowest wavelength measured (200 nm) with a maximum at 217 nm and a minimum at 234 nm in the carbonyl region as well as a positive Cotton effect in the aromatic region centered at 393 nm.

The CD analysis of compound **4** turned out to be somewhat surprising. The unheated sample of **4** was seen to have the strongest CD signal of any unheated sample, with negative Cotton effects observed at 205 nm and 231 nm in the carbonyl region, but also visible are small negative Cotton effects at 329 and 391 nm in the aromatic region. Despite the fact that this compound did not form a hydrogel, the negative Cotton effect

(22) Gupta, R.K. *Polymer and Composite Rheology*; Marcel Dekker Inc.: New York, 2000.

(23) Terech Ber, P. *Busen-Ges. Phys. Chem. Chem. Phys.* **1998**, *102*, 1630−1643.

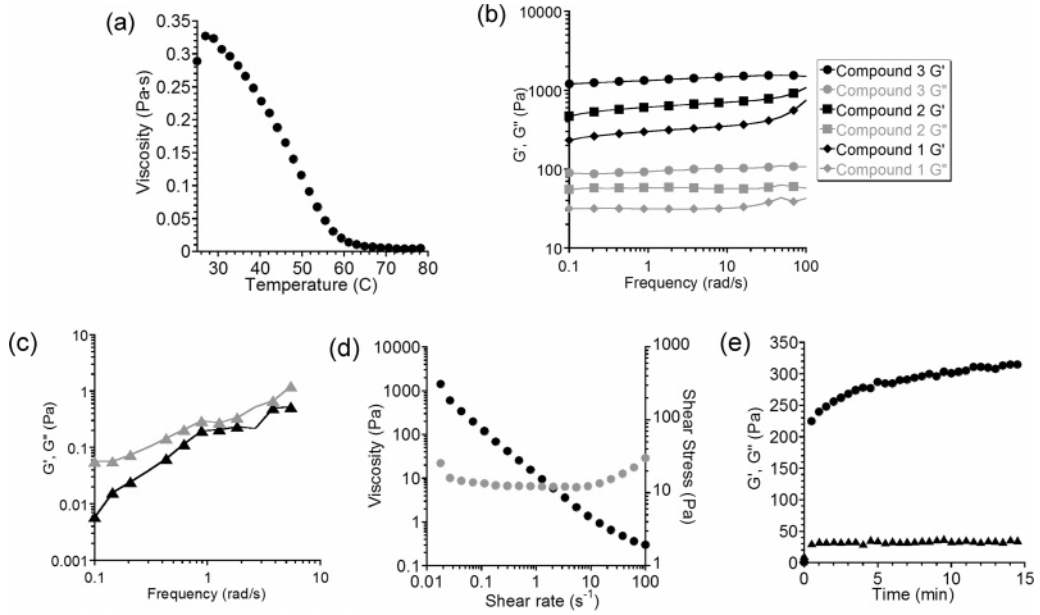

Figure 5. Rheology experiments at 4 mM concentration. (a) Viscosity measured as a function of temperature during initial ramp to 80 °C for compound **1**. (b) Frequency sweep data of storage (G' = black ◆) and loss (G'' = grey ◆) moduli for compound **1** compared to the moduli for compound **2** (G' = black ■, G'' = grey ■), and compound **3** (G' = black ●, G'' = grey ●) (c) Frequency sweep data of storage (black ▲) and loss (grey ▲) moduli for compound **4**. (d) Shear rate sweep data of viscosity (black ●) and shear stress (grey ●) for compound **1**, characteristic of a shear thinning material. (e) Recovery of gel strength after 1000% strain applied for 180 s for compound **1**.

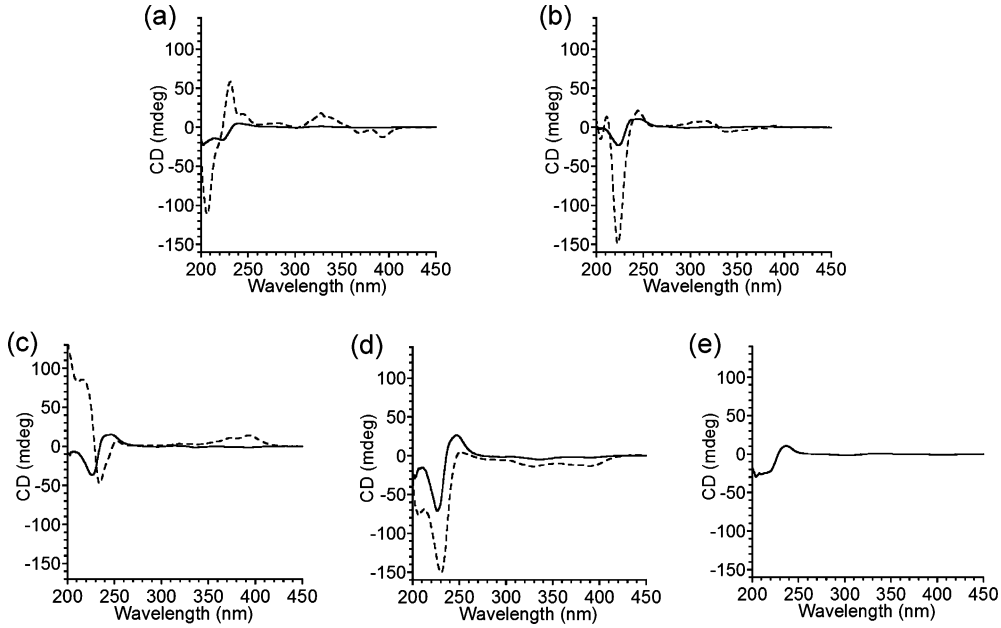

Figure 6. Circular dichroism spectra of aedamers at 0.2 mM concentration in 50 mM sodium phosphate pH=7.0, 100 mM NaCl before (—) and after (---) heating at 80 °C for 1 h. (a) Compound **1**. (b) Compound **2**. (c) Compound **3**. (d) Compound **4**. (e) Control non-amphiphilic compound **5**.

CD signals present in the unheated sample grew significantly following heating at 80 °C.

Interestingly, compound **4** showed the same more intense negative Cotton effects when incubated at 25 °C for 2 weeks as was seen following heating at 80 °C. On the other hand, samples of compounds **1**−**3** showed no change when incubated at 25 °C for 2 weeks, even after seeding with pre-gelled material.

Microscopy. Compound **1**−**3** hydrogel morphology was probed via SEM of desalted, lyophilized samples as shown in Figure 7. The SEM image of compound **1** after heating in Figure 6a shows highly branched fibers that form a three-dimensional mesh-like scaffold. Compounds **2** and **3** show similar morphologies after gelling, with compound **3** displaying thicker fibers. The SEM of non-gelling compound **4** appeared as a large mass of material with no discernible fine structure.

Discussion

Similar Folding Prior to Heating. Quantitative analysis of the spectroscopic properties of unheated samples of the amphiphilic aedamers **1**−**4** is consistent with complete folding analogous to our previously reported aedamer designs. In particular, hypochromism arises from the face-centered stacked geometry of the DAN and NDI aromatic units. The extent of hypochromism is dependent on distance r as a function of $1/r^3$

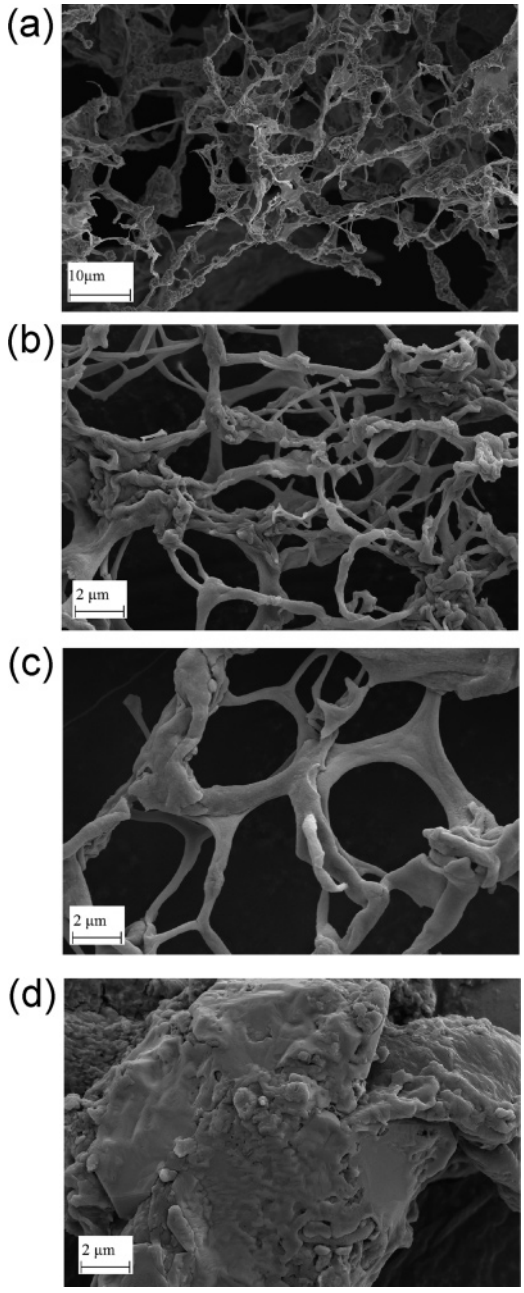

Figure 7. SEM images of gel morphology from lyophilized copper grids after heating to 80 °C. (a) Compound **1**. (b) Compound **2**. (c) Compound **3**. (d) Compound **4**. See Supporting Information for images of compound **5** as well as compounds **1**−**4** before heating.

and is highly orientation dependent with respect to the angle formed by the aromatic ring planes.[20] Prior to heating, compounds **1**−**4** exhibited nearly identical levels of hypochromism, between 51 and 53%. This similarity of hypochromism to that seen for the well-studied aedamer **5** provides strong evidence that all the amphiphilic aedamers used in this study are not only folded, they are folded to the same extent and with the same pleated, stacked conformation. For comparison, formation of the DNA double helix from DNA single strands results in an observed hypochromism of roughly 40%, the exact value of which is dependent on base sequence.[24] As further support for the folding of compounds **1**−**4**, it should be noted that they all exhibit the intense purple charge transfer absorbance (similar to the color of a fine merlot) that is characteristic of DAN-NDI stacking in water.

Aggregation and Hydrophobicity. A major difference between the amphiphilic aedamers **1**−**4** and the control aedamer **5** is that the amphiphilic aedamers aggregate in solution, as evidenced by significant viscosities prior to heating as well as their observed dynamic light scattering. Based on the dynamic light scattering data, the estimated molecular weights of the aggregates at 2.5 mM concentration are on the order of 90−400 molecules per aggregate. The control aedamer **5**, bearing 7 negative charges and no hydrophobic side chains, is monomeric in solution under these conditions.[25] Unfortunately, the aggregation prevents any detailed NMR conformational analysis of the stacked geometries of compounds **1**−**4** due to signal broadening.

The linker residues for compounds **1**−**4** were specifically chosen for their subtle geometrical differences. As a qualitative experimental measure of overall hydrophobicity, the relative retention times were compared on reversed-phase HPLC. Compounds **1**−**4** elute in the order **4** first, followed by a gap, then in quick succession: **1**, **2**, **3**. Considering that a relatively slow gradient was used (gradient increase of only 0.36% acetonitrile per minute), these differences in retention time are relatively small, consistent with the notion that overall relative molecular hydrophobicity is similar for compounds **1**−**4** (at least as it pertains to interactions with the C-18 HPLC chromatography support).

Hydrogel Formation. Analysis of compounds **1**−**5** after heating at 80 °C shows that compounds **1**−**3** form self-supporting hydrogels with varying degrees of the characteristic purple color remaining. Surprisingly, despite having an amphiphilic design similar to **1**−**3**, compound **4** did not show gelling behavior under these conditions. Control compound **5**, with only aspartic acid side chains, also showed no gelling behavior, consistent with expectations that assume amphiphilic character is a prerequisite for hydrogel formation.

The significant reduction in the charge-transfer absorbance upon hydrogel formation of compound **1** supported the original model of a "tangled" (non-ordered) state within the hydrogel, because it was assumed that any order in the hydrogel would necessarily derive from systematic donor−acceptor aromatic stacking. Relevant to the present study, an entirely non-ordered, random mode of aggregation in the hydrogel would have a statistical distribution of aromatic donor−acceptor interactions producing an average charge-transfer band that should remain relatively consistent among our series of amphiphilic aedamers. However, within the series of compounds **1**−**3**, surprising variation was seen in the retention of the charge-transfer absorbance upon hydrogel formation, ranging from 28% retention of the original charge transfer absorbance intensity for **1**, to 88% retention for **3**. This observed substantial variation indicates that differences in side chain structure are serving to strongly modulate either inter- or intra-strand aromatic donor−acceptor stacking interactions in the hydrogel state. Given the relatively subtle differences in side chain structures for **1**−**3**, it would be surprising if such large differences in aromatic stacking would be manifest in entirely unordered, tangled aggregates as originally conceived.

Viscoelastic experiments provided a more complete understanding of the material properties of compounds **1**−**3** as well as insight into the hydrogel assembly process. Compounds **1**−**3**

(24) Weissbluth, M. *Q. Rev. Biophys.* **1971**, *4*, 1−34.

(25) Zych, A. J.; Iverson, B. L. *J. Am. Chem. Soc.* **2000**, *122*, 8898−8909.

have the characteristic features of a hydrogel: frequency-independent moduli, storage modulus greater than loss modulus, and shear thinning behavior. Although compounds **1**−**3** share these characteristic features, there are significant differences in elastic behavior within the series. As a larger equilibrium storage modulus indicates a stronger, more elastic hydrogel, the trend within the series of compounds **1**−**3** indicates the isoleucine-containing aedamer **3** produces the strongest, most elastic hydrogel, followed by the norleucine-containing aedamer **2**, and leucine-containing aedamer **3**, the weakest.

A property of self-assembled gels that a polymer tangled aggregate does not share is the ability to quickly recover elastic strength after a period of strain is applied to the material.[16a,26] The hydrogel of compound **1** regained 94% of its initial elastic strength after only 15 min. This result further suggests the original non-ordered, tangled model proposed for the hydrogel self-assembly of **1** is likely not correct. In addition to the quick recovery of the gel strength, the size of the aedamers must be taken into account. Polymers often have molecular weights that are at least an order of magnitude more than compounds **1**−**4** (2.7 kD), which have a size similar to a 20−25 residue peptide. It is improbable that such small molecules forming a non-ordered tangled aggregate could hold water in a hydrogel at concentrations as low as 0.5 wt %.

Hydrogel assembly apparently begins with the disruption of the room-temperature intramolecular aggregation of folded molecules as shown by an initial decrease in viscosity upon heating. Following this loss of viscosity, hydrogel self-assembly begins (viscosity rises sharply), presumably mediated by molecules that are unfolded to some degree. The self-assembly process is apparently nucleation dependent as indicated by requirements for either (1) an air−water interface in the hydrogel chamber or (2) the seeding with a small amount of hydrogel in the absence of an air−water interface. Importantly, for **1**−**3**, hydrogel formation is accompanied by unfolding of the original pleated, stacked folded structure as evidenced by loss of the charge transfer absorbance to varying degrees. Thus, it appears that for these derivatives, hydrogel formation involves conversion to an alternative conformation.

The Hydrogels Are Derived from Highly Ordered Aggregation. The CD spectra recorded for **1**−**3** prior to heating show that the absorbing chromophores are not in a highly ordered chiral environment. In particular, the CD spectra recorded prior to heating in all cases showed minimal signal intensity, with similar peak shapes among the series, including control compound **5**, and the non-hydrogel forming amphiphilic aedamer **4**. The folded aedamer solution structure does not have obvious structural features that would be expected to give rise to strong CD signals. In particular, as opposed to a protein α-helix or β-sheet structure, the carbonyl groups in the folded aedamer backbone are relatively mobile, far apart from each other, and they interact mainly with aqueous solvent. Therefore, folded aedamer backbone carbonyls would be expected to have only minimal coupled-oscillator interactions (that are chiral) with each other, consistent with the observed relatively small signals in the far-UV region of the CD. Previous studies have indicated that stacking of the alternating aromatic units in the aedamer core involves a perpendicular arrangement of the aromatic long axes. In other words, the resulting high symmetry of the stacked core is not strongly influenced by the chiral centers of the linking chains, so again, only a small CD signal is expected in the aromatic region, consistent with what was seen.

The CD spectra for compounds **1**−**3** in the hydrogel state show significantly enhanced signals, with features that are qualitatively very different for the different compounds. The most straightforward interpretation of these observations is that hydrogel formation involves a mode of intermolecular aggregation that is highly ordered, generating a strongly chiral environment around the various chromophores, especially those in the far UV region. The linker backbone carbonyls likely make a major contribution to the far UV signals, although it should be kept in mind that absorbances centered on the aromatic units, including the carbonyls of NDI, may be making a contribution to these far-UV signals as well. The substantial differences in CD signal shapes indicate that the different compounds produce different aggregated species, despite their overall similar molecular structures and original folded conformations.

Comparison to Amyloid. The hydrogels formed from **1**−**3** can be compared to amyloid fibril formation by natural proteins. In each case, the molecule can adopt either a compact folded structure or it can be converted to a highly ordered aggregate. In the case of amyloid-forming proteins, the highly ordered aggregate state is composed of amphiphilic β-sheet structures, based on an alternating hydrophobic-hydrophilic side chain pattern. In the case of the aedamers, the exact nature of the hydrogel forming aggregate is unknown at this time. An attempt to identify infrared (IR) signatures consistent with strong hydrogen bonds involving the backbone linker carbonyl groups in the hydrogel versus solution state failed to give unambiguous results (data not shown) for **1**−**3**. What we do know is that the different compounds produced hydrogels with significantly differing amounts of DAN-NDI stacking, as indicated by the differing intensities of the visible charge-transfer bands present in each. It is not clear whether these charge transfer absorbances derive from intramolecular or intermolecular stacking or a mixture of both, so presently we are unsure of the extent to which DAN-NDI stacking is involved in the assembly process. The bottom line, however, is that like amyloid forming proteins, the CD measurements have indicated that amphiphilic aedamers **1**−**3** irreversibly form an insoluble, highly ordered aggregate. To the best of our knowledge, the amphiphilic aedamers **1**−**3** are the first folding abiotic molecules to undergo such a transition.

Branched Fibrils Lead to Hydrogel Formation. Microscopy was used to investigate the structural origin of the hydrogel properties of compounds **1**−**3**. The SEM micrographs of the hydrogels reveal networks of branched fibers surrounding relatively large cavities. The difference in gel strength and elasticity measured by rheology correlate with the thickness of the fibers in the SEM images as is most obvious when comparing the hydrogel SEM images of the norleucine (**2**) and isoleucine (**3**) derivatives. Stronger hydrogels are derived from thicker fibers. The structures of the hydrogel forming fibers seen in the SEM images for all three are branched and larger in diameter than most proteinaceous amyloid fibrils, which are generally unbranched. Apparently, the ability of heated samples of compound **1**−**3** to hold water as hydrogels arises from their branching, whereas the proteinaceous amyloids more often form insoluble precipitates.

The Valine Derivative 4. Prior to heating, the UV−vis spectra of the valine compound **4** is virtually identical to that

(26) Nowak, A. P.; Breedveld, V.; Pakstis, L.; Ozbas, B.; Pine, D. J.; Pochan, D.; Deming, T. J. *Nature* **2002**, *417*, 424−428.

of **1**−**3** indicating similar folding in solution. However, following heating, **4** does not form a hydrogel like **1**−**3**. The CD spectra taken before and after heating indicates that heating extends the order within samples of **4**, and this increase in order appears to be irreversible, like the others. As opposed to the other three, however, high temperature is not required to increase order, as incubation of **4** at room temperature for an extended period leads to the same increase in order seen following heating at 80 °C. The SEM image of heated material reveals that **4** does *not* form a branched fibrillar network like the other three. This may be a reflection of lower association energies between molecules of **4** following heating, and/or perhaps a different geometry of association that does not lead to branched fibrillar networks, which are presumably required for hydrogel formation. The bottom line is that the subtle change in chemical structure of **4**, having one -CH_2- group less in each of the three hydrophobic side chains as compared with compounds **1**−**3**, is enough to have a dramatic influence on the properties of the aggregate formed after heating. Therefore, it appears that the appearance of hydrogel properties is exquisitely sensitive to the nature and probably geometry of intermolecular aggregation that occurs upon heating.

Interestingly, both the UV−vis spectra and CD measurements indicate that **4** does not rearrange its core stacking as it produces a more ordered aggregate, because the charge-transfer band remains strong and the CD spectral features maintain the same appearance, but are amplified, with heating or when left at room temperature for extended periods. Compounds **1**−**3** show various degrees of loss of the charge-transfer band, require heating, and have altered CD spectral features following conversion to the more ordered aggregate following heating. A reasonable conclusion is that **1**−**3** undergo more significant core stacking reorganizations when the initially folded state transitions to the ordered, hydrogel-forming aggregate. This requirement for an alternative conformation may explain why **1**−**3** must be heated to produce the ordered aggregate, while **4** does not.

Kinetic and Thermodynamic Considerations. In all cases **1**−**4**, the common behavioral feature is that initial aggregation of the folded aedamers in solution gives way to the irreversible formation of a more highly ordered aggregate upon heating (or just standing in the case of **4**). The irreversible nature of this transition could be a reflection of either kinetic or thermodynamics effects or a combination of both. If the highly ordered state is the thermodynamically most stable form of the material, it is reasonable to propose that some sort of cooperative interactions between chains occurs that overcomes the significant entropic barrier imposed by ordered assembly.

Subtle Structural Differences Lead to Large Differences in Properties. Having only three examples of molecules capable of forming hydrogels makes any correlation between structure and properties preliminary. Nevertheless, interesting trends were observed for **1**−**3**. In the order **1** then **2** then **3**, retention of the charge-transfer absorbance in the hydrogel state increases, as does elastic hydrogel strength. It is tempting to propose that the increased residual charge transfer absorbance in the hydrogel formed from **3** is providing stronger associations between strands, but we cannot tell the difference between intramolecular and intermolecular stacking so such speculation is risky.

The hydrogel properties trend is also mirrored in the HPLC retention times on a C-18 column, in that **1** eluted first, then **2**, and **3** eluted last. To the extent that the HPLC retention times reflect relative molecular hydrophobicities, the implication is that increasing linker side chain hydrophobicity leads to enhanced interactions between molecules in the hydrogel state, thus offering another possible explanation for the increased elastic strength of the gels formed from **3**, with **2** and **1** having intermediate and the least elastic strength, respectively.

The relative HPLC retention times can be compared to the calculated hydrophobicities for the different side chains. Using a simple surface calculation (Spartan 04, side chains only) gives hydrophobic surface area values for valine (112 Å^2), isoleucine (132 Å^2), leucine (133 Å^2), and norleucine (137 Å^2). Using a semiempirical method based on accessibility of hydrophobic surface area within protein structures, Karplus reports values for valine (135 Å^2), isoleucine (155 Å^2), and leucine (163 Å^2).[27] Using this same approach, we come up with a value for norleucine (165 Å^2) that is very similar to leucine. Using either approach, valine is less hydrophobic by a wider margin, as isoleucine, leucine, and norleucine are relatively similar. This trend can be used to explain the reversed phase HPLC elution order of **4** (valine) followed by a gap then **1** (leucine), **2** (norleucine), then **3** (isoleucine) in quick succession. Note that the elution order of the **1**, **2**, and **3** does not exactly follow from calculated hydrophobic surface area considerations alone.

It is important to keep in perspective the relative differences seen with **1**−**3** before and after heating. The structural differences between the molecules are subtle, because **1**−**3** are in reality constitutional isomers. Consistent with the subtle nature of the structural differences, their HPLC retention times using a slow gradient are very similar. Prior to heating, their UV−vis spectra, which provide an accurate assessment of folding, are also virtually identical.

In contrast, following hydrogel formation, **1**−**3** can be easily distinguished on the basis of their hydrogel properties, CD spectra, and residual charge transfer absorbances. In other words, the aggregation that occurs upon heating amplifies tremendously the small structural differences between the molecules, a phenomenon that is best explained by proposing a highly ordered aggregate state conceptually analogous to protein derived amyloid formation. Taking a global view, our results indicate that amyloid-like behavior, namely the existence of a stably folded state as well as the irreversible formation of a highly ordered aggregate involving an alternative conformation, is not unique to proteins, but may be a relatively general property of amphiphilic folding molecules in aqueous solution. Efforts are currently underway to characterize in detail the structures of the ordered aggregates of **1**−**4**.

Acknowledgment. We thank Chris Bielawski for reading the manuscript prior to submission. This work was supported by the National Institutes of Health (GM-069647) and a grant from the Welch Foundation (F-1353).

Supporting Information Available: Experimental methods, synthetic details and characterization of compounds **1**−**4**, SEM images of compounds **1**−**4** before heating, and additional rheology data. This material is available free of charge via the Internet at http://pubs.acs.org.

JA0780840

(27) Karplus, P. A. *Protein Sci.* **1997**, *6*, 1302−1307.